

Enhancing Herbal Medicine-Drug Interaction Prediction Using Large Language Models

Sisi Yuan D, Zhecheng Zhou, Xinyuan Jin D, Linlin Zhuo D, and Keqin Li D, Fellow, IEEE

Abstract—Investigating potential interactions between drugs and herbal medicines helps optimize combined treatment strategies and supports personalized and precision medicine. Deep learning-based methods have been successful in predicting drug-related interactions. However, these methods face challenges such as low data quality and uneven distribution. Large language models (LLMs) effectively address these challenges through their extensive knowledge bases. Motivated by this, we integrate LLMs, one-hot encoding, and variational graph autoencoders (VGAEs) to propose a herbal medicine-drug interaction (HDI) prediction model. First, LLMs are employed to extract features from drug SMILES, generating high-quality molecular representations. Second, one-hot encoding is applied to herbal medicines with multiple natural products to construct feature vectors and improve model interpretability. Finally, VGAEs are utilized to reconstruct herbal medicine-drug graphs and predict unknown HDIs. Additionally, we differentiate between herbal medicine-drug similarity and the degree of individual drug or herbal medicine nodes to mitigate the dominance of high-degree nodes in VGAE message flow. Multiple experiments were conducted to validate the significance of the proposed model and its key components. This method shows great potential for applications in traditional Chinese medicine formulation optimization, new drug development, and precision medicine.

Index *Terms*—Herbal medicine-drug interaction (HDI), large language models (LLMs), variational graph autoencoders (VGAEs), uneven distribution.

I. INTRODUCTION

TERBAL medicine is fundamental to traditional Chinese medicine (TCM) theory, with its efficacy often relying on the synergistic effects of multiple components [1]. The preparations of TCM compounds are complex and diverse, comprising multiple components of plants, animals, or minerals that achieve

Received 19 December 2024; revised 10 March 2025; accepted 25 March 2025. Date of publication 7 April 2025; date of current version 7 October 2025. (Corresponding authors: Xinyuan Jin; Linlin Zhuo.)

Sisi Yuan is with the College of Computer Science and Software Engineering, Shenzhen University, Shenzhen 518060, China, and also with the Department of Bioinformatics and Computational Biology, University of North Carolina at Charlotte, Charlotte, NC 28223 USA.

Zhecheng Zhou, Xinyuan Jin, and Linlin Zhuo are with the School of Data Science and Artificial Intelligence, Wenzhou University of Technology, Wenzhou 325035, China (e-mail: jinxy@wzu.edu.cn; zhuoninnin@ 163.com).

Kegin Li is with the Department of Computer Science, State University of New York, New Paltz, NY 12561 USA.

Our code and data are accessible at: https://github.com/sisyyuan/HDI. Digital Object Identifier 10.1109/JBHI.2025.3558667

therapeutic effects through specific compatibility [2]. Unlike modern drugs that typically act on a single target, the multicomponent and multitarget characteristics of herbal medicine provide unique advantages in the treatment of complex diseases [3]. With advances in modern medicine, an increasing number of patients use herbal medicines along with modern drugs, raising concerns about potential interactions [4]. HDIs may alter drug metabolism, distribution, and excretion, impacting both the efficacy and safety of treatments [5]. For example, certain components of herbal medicines can enhance or inhibit the metabolic enzyme activity of specific drugs, altering drug concentrations in the body and thus affecting therapeutic effects or causing adverse reactions [6]. Identifying potential HDIs is essential for ensuring safe clinical drug use. The complex composition of herbal medicines means their interactions with modern drugs remain insufficiently studied. Identifying potential HDIs is crucial for ensuring drug safety in clinical practice. Traditional TCM research methods predominantly depend on empirical knowledge and qualitative approaches, including clinical effect observation and herbal combinations derived from centuries of practice. However, these methods frequently lack quantitative data, reproducibility, and standardized protocols, limiting their precision in identifying and understanding herbal ingredient interactions and their mechanisms of action [7]. Moreover, the complexity and variability of herbal formulations hinder standardization efforts and accurate assessment of their therapeutic potential [8]. The intricate composition of herbal medicines results in incompletely understood interactions with modern drugs. Developing computational models for HDI prediction enables rapid identification of potential risks from combined drug use, supporting clinical decision-making and advancing integrated Chinese-Western medicine research.

The rapid advancements in artificial intelligence (AI) and machine learning (ML) technologies have significantly accelerated progress in biomedicine. In biological network interaction prediction, computational models effectively predict and elucidate complex regulatory mechanisms. For example, Wei et al. employed a sampling method and graph neural networks (GNNs) to predict unknown non-coding RNA-protein interactions [9]. Subsequently, Zhou et al. utilized a Transformer model to extract features from k-mer sequences of non-coding RNA (ncRNA) and proteins, which were concatenated to represent ncRNA-protein pairs. The scores of ncRNA-protein pairs were then predicted by stacking multiple fully connected networks, allowing the identification of potential interactions [10]. Zhou et al. incorporated a random masking strategy based on the

2168-2194 © 2025 IEEE. All rights reserved, including rights for text and data mining, and training of artificial intelligence and similar technologies. Personal use is permitted, but republication/redistribution requires IEEE permission. See https://www.ieee.org/publications/rights/index.html for more information.

Bernoulli distribution into a graph autoencoder, proposing the JMSS-MMA model [11]. The model employed a degree decoder to learn node structures, further enhancing node representations. In a similar line of work, Xu et al. applied a semi-supervised graph autoencoder model to miRNA-disease networks, uncovering potential miRNA-disease interactions [12]. They utilized variational autoencoders and graph embedding techniques for tasks like molecular network reconstruction, demonstrating high usability and performance [13]. Additionally, Liu et al. constructed heterogeneous graphs and employed metapaths and contrastive learning techniques to predict potential circRNA-disease associations [14]. These methods not only show strong performance but also inspire new research directions, offering valuable tools to advance biomedical science.

Similarly, numerous efficient computational models have been developed for drug development and repositioning [15], [16], [17], [18]. For example, Li et al. proposed the MS-EDM model for miRNA-based drug discovery, introducing an efficient similarity fusion strategy to model the miRNA-drug graph topology from multiple perspectives [19]. Zhou et al. proposed the JDASA-MDR model to predict microbial-drug interactions, addressing the "over-smoothing" problem caused by message passing on the entire graph. The model improves prediction accuracy by extracting local features through subgraph feature enhancement [20]. In the context of drug-protein interaction prediction, Zhou et al. employed an energy-constrained diffusion mechanism to extract global features and used subgraphs to extract local features, yielding high-quality drug and protein node representations and enhancing prediction accuracy [21]. Additionally, Wei et al. proposed a drug-target interaction prediction method leveraging an integrated deep learning framework to reduce excessive false negatives [22]. Han et al. introduced a tensor decomposition method combined with deep neural networks to develop the CTF-DDI model, providing a robust tool for accurately predicting drug-drug interactions [23].

The aforementioned models demonstrate strong performance in interaction prediction and offer valuable insights for drugrelated interaction prediction tasks. However, their performance is constrained by several limitations. First, these models heavily rely on high-quality data features, which are often difficult to obtain due to data scarcity or inherent noise. Second, They rely on feature extraction techniques tailored to specific datasets, such as similarity fusion. As a result, biases within particular datasets can lead to features that lack generalizability, thereby reducing the models' ability to generalize across different contexts. Additionally, these models face challenges in interpretability. Although they perform well in drug-related interaction prediction, they often function as "black boxes," producing predictions without detailed explanations. This lack of interpretability hinders the understanding of the reasoning behind predictions, increasing the risk of false negatives and false positives, and limiting the models' practical applicability in real-world scenarios.

We propose a novel model that integrates LLM, one-hot encoding, and VGAE technologies to address the aforementioned challenges. First, LLMs are employed to extract shared features from the SMILES sequences of drugs and herbal medicine components, thereby mitigating challenges such as data scarcity

and noise. Next, K-Means clustering is applied to the features extracted by the pre-trained model for herbal components, and one-hot encoding is subsequently utilized to generate the initial features for herbal medicines. Finally, a VGAE model incorporating decoupling technology is employed to reconstruct the herbal medicine-drug graph and predict unknown HDIs. This decoupling technology reduces the dominance of high-degree nodes, thereby enhancing the interpretability of the model. To further enhance performance, we differentiate between herbal medicine-drug similarity and the degree of individual drug or herbal medicine nodes, thereby minimizing the influence of high-degree nodes on message propagation within the VGAE. Overall, our contributions are as follows:

- LLM technology is introduced to extract common features of drugs and the natural products in herbal medicines, effectively addressing challenges related to data scarcity and noise.
- A novel feature extraction method for herbal medicines is proposed, integrating K-means clustering and one-hot encoding to generate high-quality representations.
- A VGAE with decoupling technology is introduced to reconstruct the herbal medicine-drug graph, mitigating the dominance of high-degree nodes in VGAE message flow.
- 4) The HDI dataset, extracted from the Diet-Drug Interaction Database (DDID), is made freely accessible on GitHub. A series of experiments conducted on this dataset validate the effectiveness of the proposed method and its key components.

This study proposes a model to accurately predict potential HDIs. Section I provides a brief introduction to herbal medicines, reviews methods for predicting drug-related interactions, and analyzes the challenges in HDI prediction. Section II details the dataset collection process, the architecture of the proposed model, and the key components. Section III outlines the implementation of the proposed method and presents comparative experiments to validate the model's effectiveness. Additionally, ablation experiments are conducted to analyze the contribution of each key component, while parameter experiments and case studies evaluate the model's stability and robustness. Section IV provides a detailed discussion of the proposed method and an analysis of the experimental results. Section V summarizes the findings and contributions of the study.

II. MATERIALS AND METHODS

This study aims to predict the labels of unknown herbal medicine-drug pairs using observed HDIs. We integrate LLMs, one-hot encoding, and VGAE techniques to propose a model designed to accurately identify potential HDIs. **This study differentiates from similar research in two key aspects.** First, a novel method is adopted to extract initial features of herbal medicines. Specifically, LLMs are employed to extract common features of natural products in herbal medicines, followed by K-means clustering and one-hot encoding to generate initial representations. Second, we incorporate a VGAE with decoupling technology to reconstruct the herbal medicine-drug graph, addressing the issue of high-degree nodes dominating the

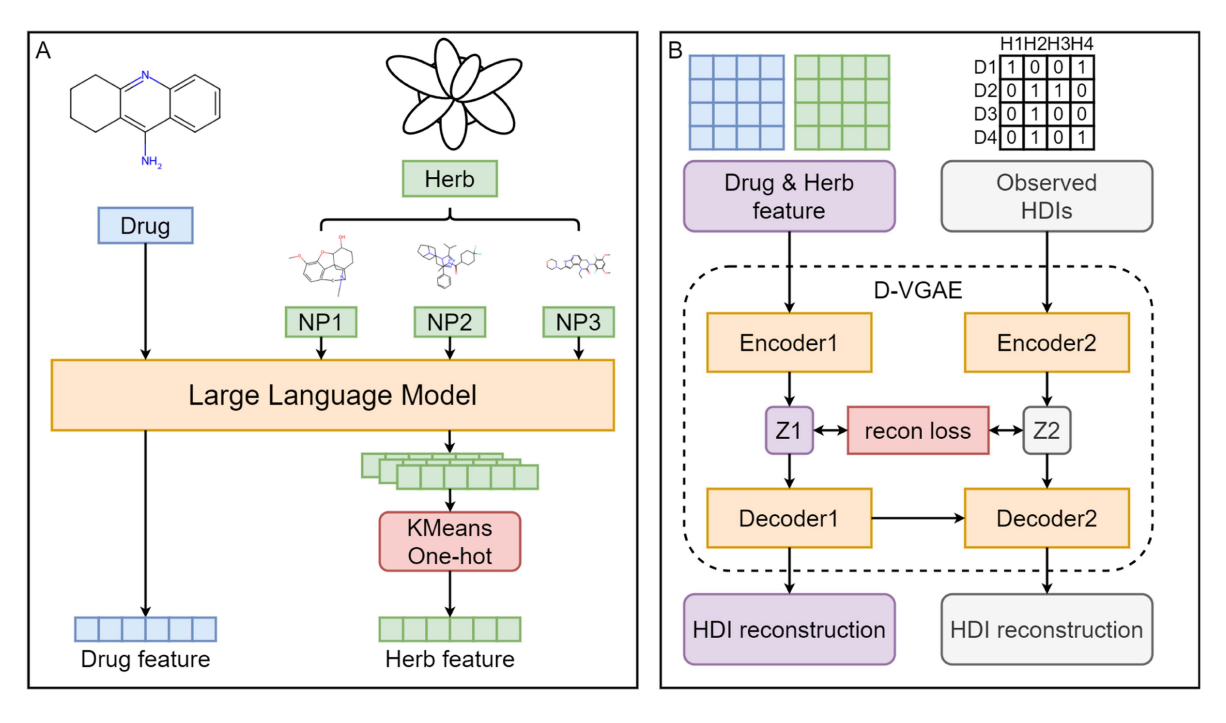


Fig. 1. The proposed model architecture consists of two primary modules: (a) Feature extraction and (b) Herbal medicine-drug graph reconstruction. In Module A, natural product (NP) features in herbal medicines and drug features are extracted from SMILES sequences using LLMs. Subsequently, K-means clustering and one-hot encoding techniques are applied to integrate NP features and generate initial herb representations. In Module B, initial drug and herb features, along with the known herbal medicine-drug adjacency matrix, are fed into the D-VGAE model [25] to reconstruct the herbal medicine-drug graph. The D-VGAE model initially attempts to predict HDIs based on herbal medicine-drug similarity. If unsuccessful, it then attempts to predict interactions in node neighbor density case. NP refers to natural products. Encoder1 and Encoder2 correspond to encoders based on herbal medicine similarity and node neighbor density, respectively.

message flow in VGAE. Next, we present detailed statistics of the extracted HDI dataset. Finally, we will describe the principles and techniques behind the key modules of our model.

A. Data Preparation

The data for this study were primarily sourced from the latest DDID database [24], which compiles data from literature, FDA labels, and various online repositories. The database includes 1,338 foods and herbal medicines (from plant and animal sources), 1,516 widely used drugs, and 23,950 interaction records. These interactions are categorized into fooddrug interactions and HDI. For HDI, DDID includes 1,068 herbal medicines from 155 families, along with their respective natural products. This study focused on HDIs, filtering out incomplete data and retaining only drug names and SMILES, herbal medicine names, and their associated natural products with SMILES. Ultimately, 7,591 HDI records were obtained, encompassing 1,424 drugs, 681 herbal medicines, and 43,517 natural products. The extracted dataset has been made publicly available on GitHub for free access.

B. Model Overview

Fig. 1 illustrates the architecture of the proposed model, which consists of two main modules: (A) Feature extraction and (B) Herbal medicine-drug graph reconstruction. In module A, drugs, natural products of herbal medicines, and their corresponding HDIs are obtained from the DDID database. Subsequently, initial features are extracted from the SMILES sequences of

the natural components in herbal medicines and the drugs using the LLM technique. Additionally, K-means clustering and one-hot encoding are applied to the natural products of herbal medicines to generate their initial features. In module B, the feature matrices of drugs and herbal medicines, along with the known herbal medicine-drug adjacency matrix, are initially input. Subsequently, the herbal medicine-drug adjacency matrix is reconstructed using an encoder-decoder architecture under herbal medicine-drug similarity measures and node degree information, respectively.

C. LLM Technology for Initial Feature Extraction

LLM technology has achieved significant success in computer vision [26], natural language processing [27], protein sequence analysis [28], and other domains. This advancement has indirectly facilitated the application of LLM technology in representing compound SMILES sequences. In drug-related interaction prediction, current models typically employ two approaches to generate initial node representations. First, many models rely on observed adjacency matrices to directly calculate similarity. This approach selectively ignores unknown elements in adjacency matrices, inevitably introducing bias [29]. Second, some models utilize convolutional neural networks, GNNs, or Transformers to extract node representations. This dependency often ties extracted node representations to downstream tasks, limiting model generalization [30]. Fortunately, several pre-trained models based on SMILES sequences have been developed recently, helping to mitigate these issues.

This study extracted SMILES sequences of natural products in herbal medicines and the drugs from DDID, enabling pre-trained models to directly generate their initial representations. Specifically, ChatGPT [27] was selected for representation generation. Like the BERT model, ChatGPT employs a stacked Transformer architecture. ChatGPT, a large language model trained to process sequential data, was employed to interpret SMILES sequence syntax and semantics in this study. Unlike traditional methods that rely on manually crafted features or predefined rules, ChatGPT automatically captures complex relationships among atoms, bonds, and functional groups in SMILES sequences, enhancing its effectiveness in learning molecular structures from raw data. This capability enables ChatGPT to better comprehend both local and global structural information in chemical compounds. First, the SMILES sequence is normalized using RDKit to ensure a standardized format. Key chemical features, such as functional groups, molecular weight, aromaticity, and hydrogen bond donors/acceptors, are extracted and converted into natural language descriptions. Finally, the OpenAI API (text-embedding-ada-002) is utilized to generate embeddings from the text descriptions, with a default dimensionality of 768. For drugs, these initial representations are directly used as input for subsequent models.

D. Feature Extraction of Herbal Medicines

The extracted HDI dataset contains 681 herbal medicines and 43,517 natural products. Previous research [31] identifies two primary strategies for extracting herbal medicine representations. The first method calculates similarity between herbal medicines based on observed HDI data to serve as the initial representation. However, this approach neglects unknown elements in the adjacency matrix, potentially introducing bias. The second method utilizes randomly generated embeddings, but this introduces excessive uncertainty and fails to accurately capture the features of herbal medicines. To address these limitations, we propose a novel method for extracting herbal medicine representations using K-means clustering and one-hot encoding.

First, K-means clustering is applied to the 768-dimensional features of natural products output by the pre-trained model. Additionally, the number of categories is set to 768 to align with the dimensionality of the initial drug representation. As a result, the 43,517 natural products are grouped into 768 categories. Next, one-hot encoding is applied to extract initial representations of herbal medicines. Specifically, the 768 categories are sorted, with each category treated as a dimension. Let h represent a herbal medicine, d a dimension (or category) with an initial value of 0, and m a natural products. If h contains m, and m belongs to d, then the value of d is incremented by 1. Consequently, a 768-dimensional feature vector for herbal medicine is generated and input into the prediction model alongside the drug feature.

E. HDI Prediction

Based on the above feature extraction method, initial representations of drugs and herbal medicines are extracted from the HDI dataset. A model is then constructed to predict the labels

of unknown herbal medicine-drug pairs using known HDIs. GNNs have proven effective in uncovering and understanding topological structures in graph data [32]. However, compared to GNNs, graph autoencoder (GAE) technology enables self-supervised training, making it more efficient for graph reconstruction tasks, which is why it is considered a promising approach [33]. VGAE technology, in particular, generates new data from existing inputs, introducing model uncertainty and helping mitigate the impact of noise or data scarcity [34]. Furthermore, VGAE integrates regularization and learns latent probability distributions, making it highly suitable for HDI prediction tasks.

VGAE is a GNN-based generative model designed to generate node representations by learning latent variable probability distributions, enabling graph reconstruction. Similar to GAE, VGAE comprises two main components: an encoder and a decoder. In VGAE, the GNN encoder learns an approximate Gaussian distribution, and node representations are obtained through sampling. The decoder then computes the inner product of the herbal medicine-drug pair based on the provided node representations, followed by applying the sigmoid function to estimate the probability of an edge. Model training is guided by two primary optimization objectives: reconstruction loss, which quantifies the difference between the predicted and actual labels of herbal medicine-drug pairs; and KL divergence, which measures the divergence between the learned latent probability distribution and the normal distribution.

Studies have demonstrated that in GNNs, high-degree nodes can dominate information flow propagation when neighborhood density varies significantly [35]. This issue is also evident in the herb medicine-drug interaction graph. To address this issue, we employ DVGAE [25], a variant of the Variational Graph Autoencoder (VGAE) based on decoupling technology, to enhance HDI prediction. The key of DVGAE lies in decoupling node representations into two components: node similarity and neighborhood density (degree). First, a high similarity between two nodes suggests a higher probability of interaction. Second, high-degree nodes are often more popular, thereby increasing the likelihood of interactions with other nodes. This dual feature encoding improves the model's ability to capture complex interactions between drugs and herbal medicines, which is essential for accurate HDI prediction. The key technologies and principles are elaborated in the following sections.

1) Graph Normalized Convolutional Network: The DVGAE framework employs a Graph Convolutional Network (GCN) encoder to approximate the Gaussian distribution. DVGAE uses node similarity and neighborhood density to guide the reconstruction of the herbal medicine-drug graph. Consequently, the GCN encoder generates two sets of similar probability distributions. One set represents herbal medicines (or drugs) based on herbal medicine-drug similarity (μ^s, Σ^s) , while the other represents them based on neighborhood density (μ^d, Σ^d) . This idea comes from the fact that the degree of a node is a feature of the node itself. This study introduces the regularized encoder from the VGNAE framework [36], as the L2 normalization method mitigates issues caused by sparse neighborhoods disrupting gradient propagation. Specifically, a graph normalized

convolutional network (GNCN) [36] is proposed:

$$GNCN(X, A, c) = cDiag(A)^{-\frac{1}{2}}ADiag(A)^{-\frac{1}{2}}f(XW), \tag{1}$$

where A denotes the adjacency matrix, while Diag(A) denotes the diagonal matrix derived from A. And $f([z_1, z_2, \ldots, z_n]^T) = [\frac{z_1}{\|z_1\|}, \frac{z_2}{\|z_2\|}, \ldots, \frac{z_n}{\|z_n\|}]^T$, W represents a learnable parameter matrix, and c is a tuning factor typically set to 1.8.

2) Decoupling-Based Generation Process: In the herbal medicine-drug graph G=< H, D, E>, H denotes the set of herbal medicine nodes, D the set of drug nodes, E the observed HDIs, and E is the adjacency matrix derived from E. Each herbal medicine (or drug) is assumed to interact with drugs (or herbal medicines) under two conditions: high node similarity or high node degree. Instead of randomly selecting a condition to determine interactions for each herbal medicine-drug pair, a Bernoulli distribution is used to sample conditions for establishing interactions. Specifically, the probability distributions (μ^s, Σ^s) and (μ^d, Σ^d) of herbal medicines (or drugs) under these two conditions are derived from the GNCN encoder. Subsequently, herbal medicine (or drug) representations are generated by sampling from two Gaussian distributions:

$$h_u^s \sim \mathcal{N}(\mu^s, \Sigma^s), h_u^d \sim \mathcal{N}(\mu^d, \Sigma^d),$$
 (2)

where $u \in H \cup D$, \mathcal{N} denotes a Gaussian distribution. Let i represent a herbal medicine and j a drug. For the < i, j > pair, Bernoulli sampling is used to determine the condition for generating an interaction. The process begins by attempting to generate an interaction based on herbal medicine-drug similarity:

$$A_{ij} \sim Bernoulli(\sigma(sim(h_i^s, h_i^s))),$$
 (3)

where σ represents the sigmoid function, and sim() denotes the cosine similarity measurement function. h_i^s and h_j^s denote the embeddings of herbal medicine i and drug j in the similarity case, respectively. If $A_{ij}=1$ is derived from (3), the interaction is established under the similarity condition, and no further attempts are made under the node neighborhood density condition. Otherwise, if $A_{ij}=0$, the interaction is evaluated based on the node neighborhood density condition:

$$A_{ij} \sim Bernoulli(\sigma(snd(h_i^d, h_i^d))),$$
 (4)

where snd() represents the node neighborhood density measurement function, which specifically counts the node degree. h_i^d and h_j^d denote the embeddings of herbal medicine i and drug j in the similarity case, respectively.

Based on the above measures, interactions for herbal medicine-drug pairs are generated independently under the two conditions through sampling. This independence ensures that high-degree nodes do not dominate the similarity-based modeling process.

F. Optimization Objectives

The model's optimization objectives primarily involve minimizing the discrepancy between the predicted and true labels of herbal medicine-drug pairs, as well as the divergence between the predicted probability distribution and the posterior Gaussian

distribution. These objectives are reformulated as optimizing the evidence lower bound (ELBO) on the variational parameter:

$$\mathcal{L}(\phi, \theta, A) \equiv \mathbf{E}_{q\phi(H^{d,s}|X,A)}[\log p_{\theta}(A|H^{d,s})]$$

$$- KL(q\phi(H^{d}|I,A)||p(H^{d}))$$

$$- KL(q\phi(H^{s}|X,A)||p(H^{s})), \tag{5}$$

where the first term represents the label prediction loss, while the second and third terms correspond to the losses associated with the probability distributions of predicted similarity and node neighborhood density, respectively. KL() measures the Kullback-Leibler (KL) divergence between two variables. H^d and H^s denote the node embeddings of drugs and herbal medicines, derived from node degree and herbal medicine-drug similarity, respectively. $q\phi(H^{d,s}|X,A)$ denotes the model that generates the node matrix $H^{d,s}$ using input features and the known adjacency matrix, given parameter ϕ . $p_{\theta}(A|H^{d,s})$ denotes the probability of generating the adjacency matrix Abased on the node matrix $H^{d,s}$. Following previous work [37], $p(h_i) = \mathcal{N}(h_i|0, I)$ is used to represent the Gaussian prior, and the posterior is assumed to approximate $q(h_i|x_i, A)$ as a Gaussian distribution. Notably, the GNN encoder uses I instead of Xas input (see the second term in (5)) to guide the generation of the probability distribution based on node neighborhood density. This approach is adopted because node neighborhood density is an intrinsic feature of the node itself, eliminating the dependency on X. The first term is expressed as follows:

$$\mathbf{E}_{q\phi(H^{d,s}|X,A)} \log p_{\theta^s}(A|H^s) p^s + \mathbf{E}_{q\phi(H^{d,s}|X,A)} \log p_{\theta^d}(A|H^d) p^d, \tag{6}$$

where $p_{\theta^s}(A|H^s)$ and $p_{\theta^d}(A|H^d)$ are derived from (3) and (4), respectively, and p^s and $q^s = 1 - p^s$ are Bernoulli parameters, representing the probabilities of establishing interactions based on similarity and node neighborhood density, respectively.

Subsequently, the optimization process based on the EM algorithm is completed following the "winner-take-gradient" training strategy [38]. The detailed procedure is provided in [39].

III. RESULTS

A. Experimental Settings

This study evaluates the performance of the proposed method and comparative methods using the extracted HDI dataset. Comparative methods include common approaches such as MLP, GCN [40], GAT [41], and specific interaction prediction models like CTF-DDI [23], DPI-GLP [21], MS-EMD [19], and JDASA-MDR [20]. The extracted HDI dataset is split into training, validation, and test sets with an 8:1:1 ratio. Negative samples, equal in number to positive samples, are selected from unknown herbal medicine-drug pairs, ensuring no duplicate data. To ensure fairness, the same data partitioning is applied across all methods. The initial drug features for all models are obtained from the proposed model. The proposed method employs one-hot encoding to extract features of herbal medicines, whereas other methods utilize randomly generated features. The model dimension is set to 256, with a scaling factor of 1.8. The Adam

Methods/Metrics	AUC	AUPR	ACC	SEN	PRE	SPE	F1-score
MLP GCN	78.75 92.66	74.83 91.77	67.92 87.55	53.89 92.75	74.91 84.01	81.95 82.35	62.68 88.17
GAT	92.64	92.42	71.34	93.54	64.78	49.14	76.55
CTF-DDI DPI-GLP	83.12 94.50	77.65 96.78	77.10 93.18	95.02 91.70	69.96 94.50	59.19 94.66	80.58 93.08
JDASA-MDR	96.74	96.98	92.14	93.24	91.23	91.04	92.23
Mask GAE Ours	97.39 98.48	96.90 98.21	92.53 95.20	93.19 94.53	91.97 95.81	91.86 95.87	92.58 95.17

TABLE I
RESULTS OF ALL MODELS ON THE HDI DATASET (%).

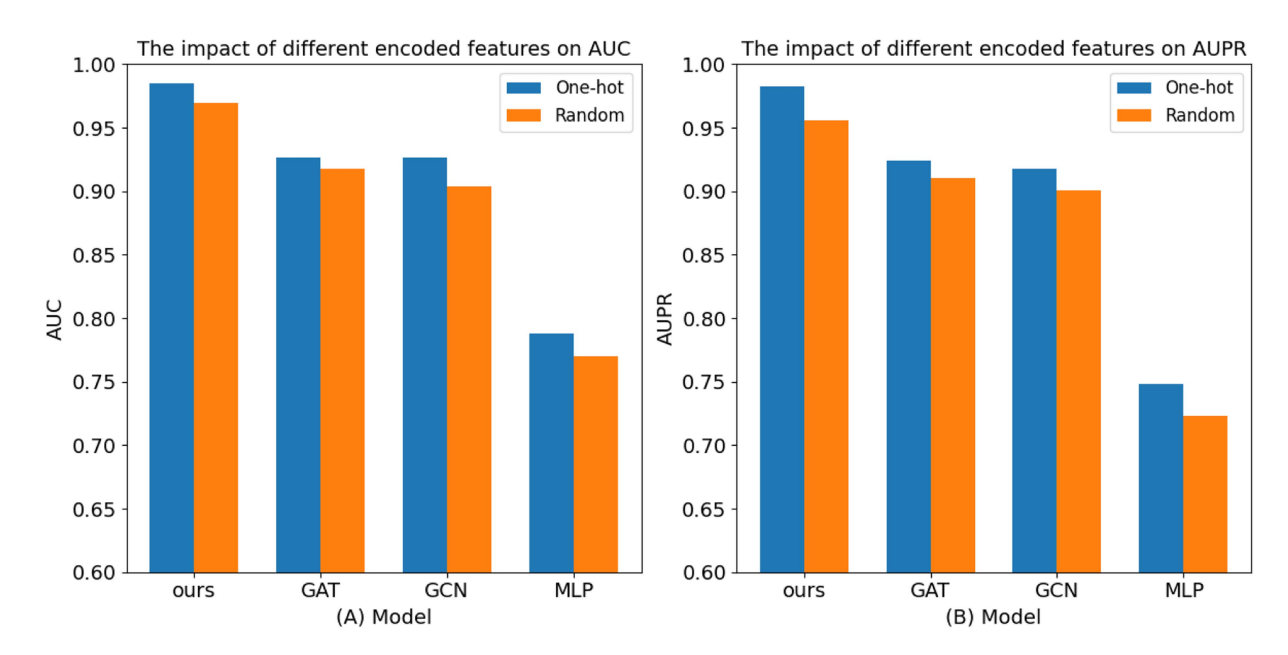


Fig. 2. AUC and AUPR Performance of ablation experiments.

optimizer is employed during training, and the learning rate is fixed at 0.01. Performance is evaluated using AUC, AUPR, accuracy (ACC), sensitivity (SEN), precision (PRE), specificity (SPE), and F1-score as indicators [42], [43], [44] for the proposed method and comparative methods.

B. Performance Comparison

The performance of all methods was evaluated on the HDI dataset, with results presented in Table I. MLP and CTF-DDI, which do not utilize GNN technology, exhibited the poorest performance, whereas models incorporating GNN technology performed significantly better. This can be attributed to GNN's capability to capture the topology of the herbal medicine-drug graph, allowing for more accurate representation of relationships between unknown herbal medicine-drug pairs. The DPI-GLP model extracts global features from the herbal medicine-drug graph and accounts for potential dependencies among herbal medicine-drug pairs that are not directly connected. By extracting local features, DPI-GLP mitigates the "over-smoothing" issue typically encountered in message propagation mechanisms, thus improving the identification of potential HDIs.

JDASA-MDR integrates self-supervised training and masking strategies, further boosting its performance. Notably, the proposed method outperformed all other models, achieving 98.48% AUC, 98.21% AUPR, 95.20% ACC, 94.53% SEN, 95.81% PRE, 95.87% SPE, and 95.17% F1-score. The only slight lag was observed in the SEN metric, where it trailed CTF-DDI. These results demonstrate that the proposed method is a reliable tool for accurately identifying potential HDIs.

C. Ablation Experiments

As described in Section II-C, this study employed LLM to extract initial features from the SMILES representations of natural products in herbal medicines and the drugs. Subsequently, clustering technology and one-hot encoding were applied to extract initial features of herbal medicines from their natural products. To investigate the role of the proposed feature extraction module based on one-hot encoding, an ablation experiment was conducted. In addition to the proposed method, common models such as GAT, GCN, and MLP were also included for comparison. In Fig. 2, "One-hot" indicates that one-hot encoding was used to extract initial features of herbal medicines, while

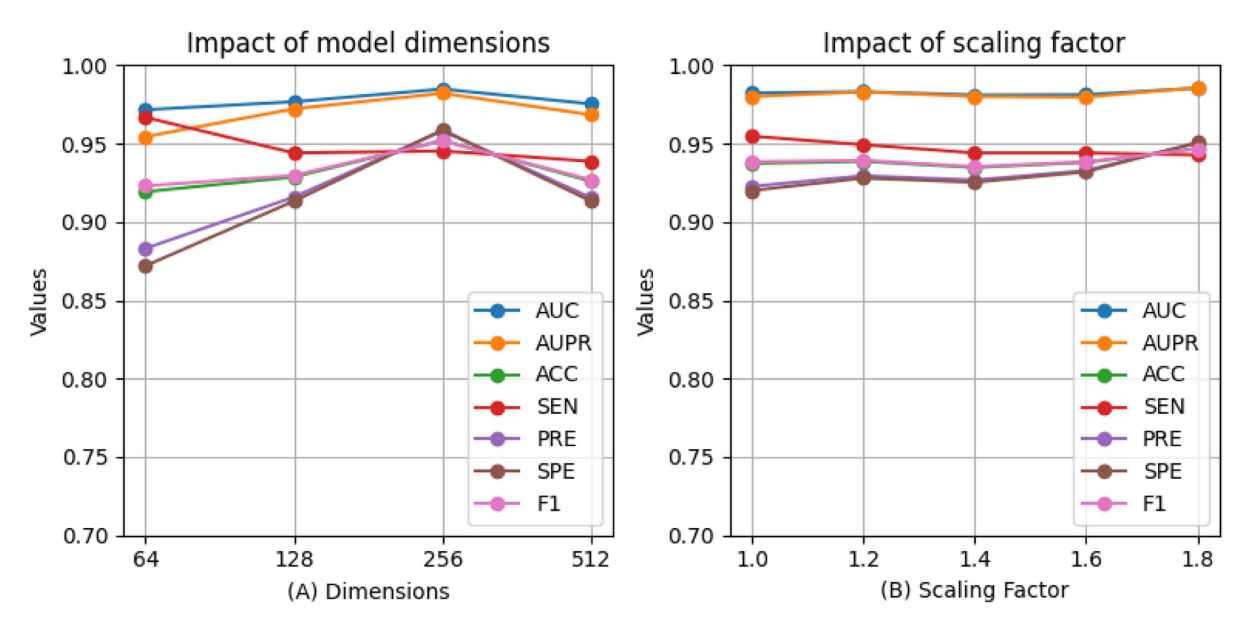


Fig. 3. Evaluating model's performance with different dimensions and scaling factors.

"Random" refers to a random method for generating initial features. The results demonstrate that the performance of all models significantly improved after adopting one-hot encoding, validating the effectiveness and rationale of the proposed feature extraction module.

D. Parameter Experiments

1) Testing Different Feature Dimensions: To evaluate the model's robustness and sensitivity to parameters, a series of experiments were designed to analyze the impact of parameter variations. Specifically, we focused on the linear transformation layer defined by (3), which maps input data to a new feature space and generates a regularized feature vector for subsequent processing. In the experimental design, a control variable method was employed, where all other parameter settings were fixed, and only the dimension size of the linear transformation layer was adjusted. The experimental results, presented in Fig. 3(a), reveal that when the dimension of this layer is set between 64 and 256, model performance steadily improves. However, when the dimension exceeds 256, model performance slightly declines. We speculate two potential reasons for this trend. On one hand, a narrow dimension may prevent the model from fully capturing key feature information; on the other hand, an excessively high dimension may introduce redundant information, hindering further performance improvement. Therefore, to ensure good generalization on new data while avoiding performance degradation, a balanced dimension size should be selected.

2) Testing Different Scaling Factor: This study evaluated the effect of variations in the scaling factor c in (3) on model stability. The scaling factor is designed to expand the feature vector after regularization. In this experiment, a control variable approach was employed, where all other conditions were fixed, and only the scaling factor was adjusted to observe its direct impact on model performance. The experimental results (Fig. 3(b)), reveal

that the model achieves optimal performance when the scaling factor is set to 1.8. When the scaling factor slightly deviates from 1.8, either increasing or decreasing, model performance marginally declines. These findings indicate that the model exhibits tolerance to variations in the scaling factor and is not overly sensitive to its specific value. This highlights the model's reliability, demonstrating its robustness and adaptability in practical applications.

3) Testing Different Input Features: Additionally, a series of parameter experiments were conducted to investigate the contribution of different drug and natural product features to the model's performance (Fig. 4). Fig. 4(a) illustrates the use of LLM technology to extract molecular fingerprint features from drugs and natural products of herbal medicines, while Fig. 4(b) demonstrates the extraction of SMILES features using LLM technology. Using the SMILES sequence yields 98.48% AUC and 98.21% AUPR, whereas using molecular fingerprints results in slightly lower results, with 97.80% AUC and 97.83% AUPR. For clarity, the clustering category was set to 20. The results of using molecular fingerprints and SMILES are shown in Fig. 4(c) and (d), respectively, while the feature distributions after PCA-based dimensionality reduction are depicted in Fig. 4(e) and (f). Notably, the results indicate that using SMILES sequences for clustering results in more distinct and separable feature representations.

4) Testing Different Clustering Methods: Owing to the complexity of natural products in herbal medicines, conventional feature extraction methods are often inadequate. Therefore, this study employs K-means clustering to group natural products in herbal medicines, followed by one-hot encoding to generate their initial representations. K-means clustering plays a critical role in this process. Several clustering methods are available, including hierarchical clustering and DBSCAN. An optimized clustering algorithm could potentially enhance model performance significantly. To explore this possibility, we implemented

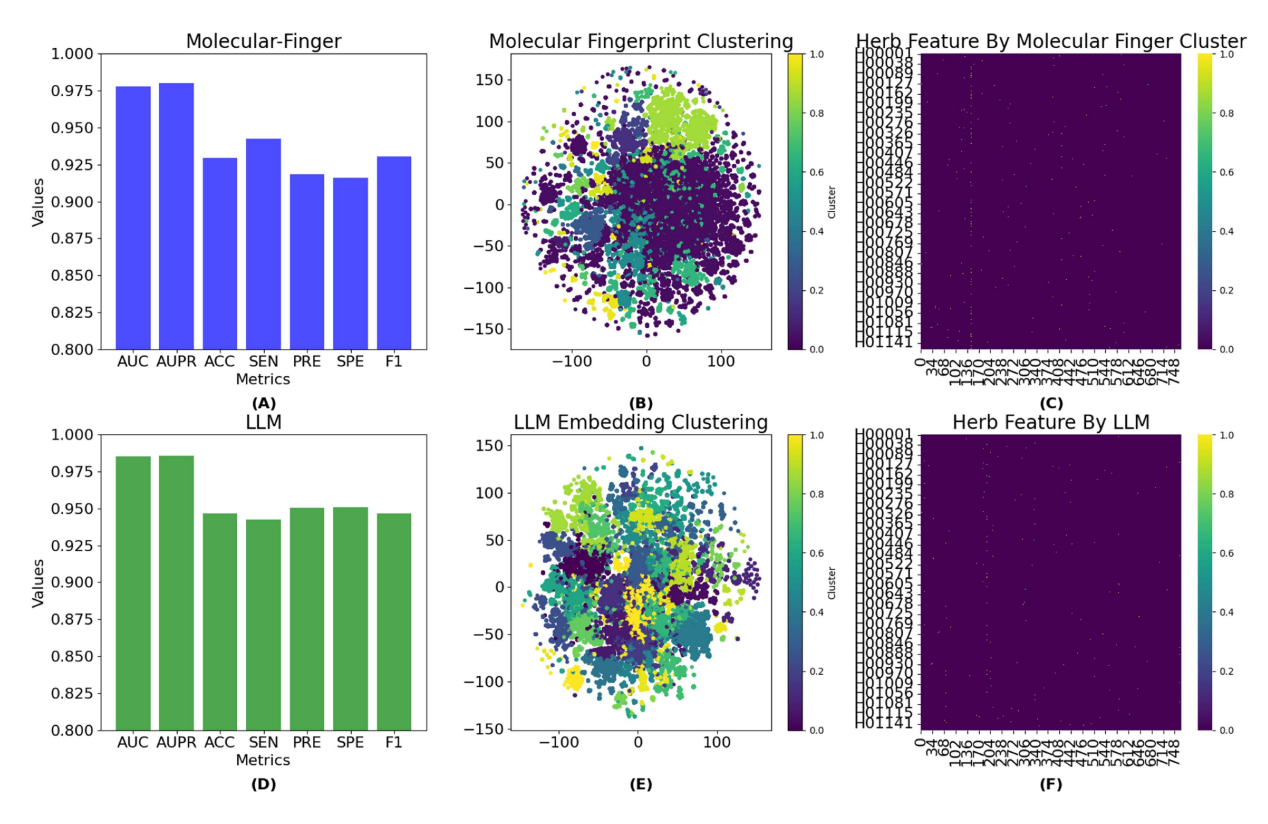


Fig. 4. Evaluating model's performance with different input features: (a) molecular fingerprint and (d) SMILES sequence. (b) and (e) represent the clustering distributions for molecular fingerprints and SMILES sequences, respectively. (c) and (f) represent the feature distributions according to molecular fingerprints and SMILES sequences, respectively.

TABLE II
EVALUATING MODEL'S PERFORMANCE WITH DIFFERENT CLUSTERING
METHODS (%).

Methods/Metrics	AUC	AUPR
Hierarchical clustering DBSCAN K-means	98.42 98.36 98.48	98.03 97.91 98.21

hierarchical clustering and DBSCAN as alternatives to K-means and conducted a comparative analysis. Table II compares the model's performance using hierarchical clustering, DBSCAN, and K-means clustering algorithms. It is evident that the choice of clustering technique has a minor impact on model performance. Therefore, a simple and practical clustering strategy can be selected based on specific requirements.

E. Performance Evaluation

To further evaluate the model's performance and reduce the impact of random errors, a five-fold cross-validation was performed on the dataset. Table III presents the detailed five-fold cross-validation results of the proposed model. The data reveal that the model achieves excellent performance metrics: an average AUC of 95.84%, an AUPR of 97.23%, an ACC of 92.01%, a PRE of 93.65%, a SEN of 90.14%, and an F1-score of 91.86%. Notably, the performance across the five validation

folds is highly consistent, with minimal fluctuations, underscoring the stability of the proposed model. This consistency further highlights its adaptability and reliability, ensuring that the model is robust and performs well under various dataset splits.

F. Case Study

St. John's Wort is a perennial herb in the Garcinia family [45]. The flowers and leaves of St. John's Wort are commonly used in herbal therapy. Its primary active ingredients, including hypericin, hyperoside, and flavonoids, are known to exhibit various biological activities, including antidepressant, antibacterial, antiviral, and anti-inflammatory effects [46]. St. John's Wort is typically used as dried herbs, capsules, tablets, tea, or tinctures. However, despite its potential health benefits, attention must be paid to possible side effects and drug interactions. St. John's Wort can alter the hepatic metabolism of certain drugs, potentially reducing their efficacy or increasing side effects, particularly when combined with antidepressants, oral contraceptives, anticoagulants, or anti-epileptic drugs. To evaluate the model's ability to predict drugs interacting with St. John's Wort, an experiment was designed. During model training phase, all drugs known to associate with St. John's Wort were excluded from the dataset. In the testing phase, St. John's Wort and all drug combinations were input into the trained model. The top 20 drugs were selected based on model-predicted probabilities, 19 of which were validated as known interactions in the database. Acebutolol was the only drug not verified in

Folds/Metrics	AUC	AUPR	ACC	SEN	PRE	SPE	F1-score
1	98.48	98.21	95.20	94.53	95.81	95.87	95.17
2	98.36	98.19	94.40	94.53	94.28	94.27	94.41
3	98.37	98.17	94.73	94.13	95.28	95.33	94.70
4	98.42	98.23	94.80	95.33	94.33	94.27	94.83
5	98.43	98.14	94.93	94.27	95.54	95.60	94.90
Avg	98.41	98.18	94.81	94.56	95.05	95.07	94.80

TABLE III
RESULTS OF THE PROPOSED MODEL ON THE HDI DATASET (%).

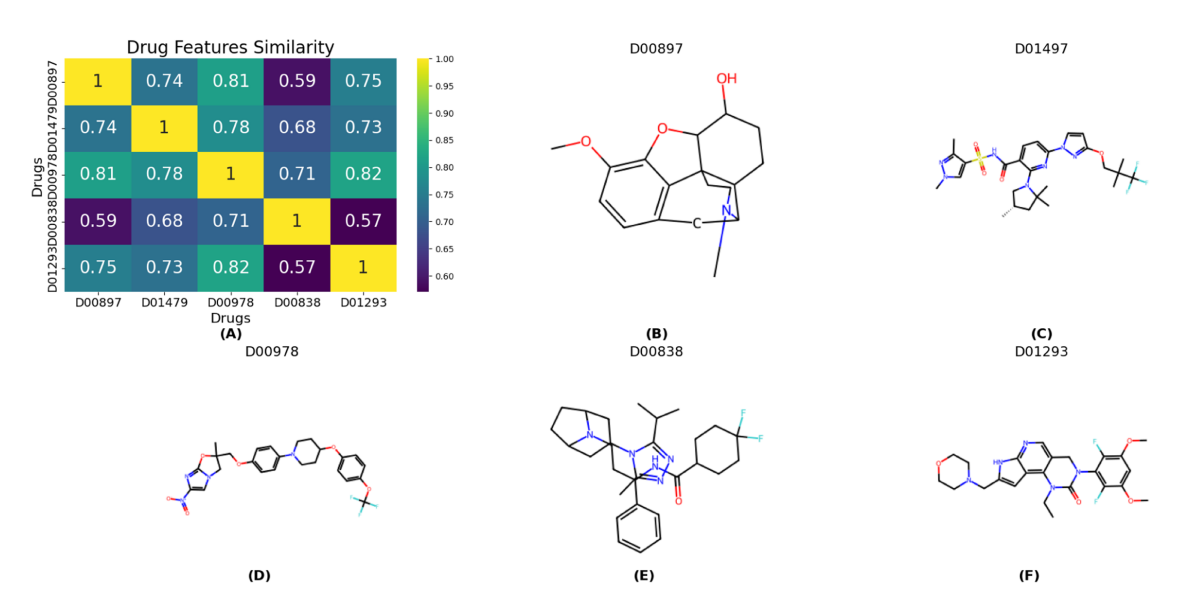


Fig. 5. (a) Similarity matrix for drugs (b) D00897, (c) D01497, (d) D00978, (e) D00838, and (f) D01293 showing the highest predicted association scores with St. John's Wort.

TABLE IV
RESULTS OF CASE STUDY (%).

Name	Score	Name	Score
Dihydrocodeine	98.40	Ivabradine	70.48
Elexacaftor	97.43	Fexofenadine	68.92
Delamanid	97.19	Dexfenfluramine	67.16
Maraviroc	96.30	Dextromethorphan	66.39
Pemigatinib	95.32	Atorvastatin	65.93
Neratinib	90.67	Pitolisant	62.63
Brexpiprazole	89.98	Voxilaprevir	62.07
Clarithromycin	83.99	Acebutolol	61.73
Cobimetinib	79.42	Ifosfamide	60.92
Doxycycline	78.70	Milnacipran	60.43

the database, as indicated in bold in Table IV. These results demonstrate the effectiveness and reliability of the proposed model in accurately identifying potential HDIs.

We selected the top five drugs with the highest scores from the prediction results: DOO897, D01497, D00978, D00838, and D01293. A similarity matrix, based on the feature vectors of these drugs, was computed and visualized as a heat map in Fig. 5(a). Additionally, the chemical structures of the five drugs were plotted using their SMILES representations in Figs. $5(b)\sim(f)$. The analysis revealed that these five compounds exhibit high similarity, with the exception of D00897 and D01293,

which show lower similarity to D00838. This suggests that structurally similar drugs may share properties, such as a higher likelihood of interacting with the same herbal medicine.

IV. DISCUSSION

Investigating potential interactions between herbal medicines and drugs facilitates the development of integrated Chinese and Western medicine treatment strategies. Currently, there are few methods available to identify potential HDIs among the vast array of herbal medicine-drug pairs. Furthermore, existing drugrelated network prediction methods have specific limitations. For instance, in the herbal medicine-drug bipartite graph, the number of neighbor nodes for drugs and herbal medicines varies significantly, leading to uneven data distribution. The limited number of known HDIs complicates the extraction of accurate and generalized node representations. Additionally, effective methods for extracting features of herbal medicines are lacking. To address these challenges, we propose a novel model that integrats LLM, VGAE, and "one-hot" encoding technologies to efficiently and reliably identify potential HDIs among extensive herbal medicine-drug pairs.

This study evaluates the proposed model's performance against several comparison models using the collected HDI dataset, demonstrating its effectiveness. Ablation experiments were conducted to validate the effectiveness of the proposed herbal medicine feature extraction module, which leverages clustering and "one-hot" encoding technologies. The results of multiple parameter experiments confirm the proposed model's robustness to varying parameter settings and the reliability of its predictions. Additionally, a series of case studies were conducted to further highlight the proposed model's exceptional performance in isolated scenarios.

V. CONCLUSION

Herbal medicine plays a central role in traditional medicine, and integrating modern medical research can significantly enhance the development of integrative medicine. A thorough investigation into the relationship between drugs and herbal medicines aids in optimizing combined treatment plans and advancing personalized precision medicine. Building on this context, this study introduces an innovative deep learning model leveraging LLM and VGAE technologies. The study first gathered and organized the HDI dataset from the latest herbal medicine-drug database. LLM technology was then employed to extract high-quality features from the SMILES representations of the natural components of drugs and herbal medicines. Concurrently, clustering and "one-hot" encoding techniques were innovatively applied to construct features derived from the natural components of herbal medicines, greatly enhancing the model's interpretability. Compared to traditional methods, the proposed model demonstrated substantial improvements in HDI prediction.

However, the model has several limitations. First, it does not incorporate 2D or 3D structural information of the natural products in herbal medicines or the drugs. Second, the dataset does not account for factors such as bias, and the random selection of negative samples may result in false negatives. In future work, we plan to employ advanced multimodal fusion techniques to integrate SMILES sequences with 2D or 3D structural information of natural products in herbal medicines or the drugs, enabling a more comprehensive representation. Second, we aim to debias the dataset and integrate relevant clinical information with LLM technology to improve the collection of negative samples, thereby minimizing false negatives. Through these improvements, the proposed model might demonstrate significant potential in various domains, such as optimizing Chinese medicine formulations, developing new drugs, planning personalized treatments, and advancing precision medicine.

REFERENCES

- X. Zhou et al., "Synergistic effects of chinese herbal medicine: A comprehensive review of methodology and current research," Front. Pharmacol., vol. 7, 2016, Art. no. 201.
- [2] A. Zhang, H. Sun, and X. Wang, "Potentiating therapeutic effects by enhancing synergism based on active constituents from traditional medicine," *Phytotherapy Res.*, vol. 28, no. 4, pp. 526–533, 2014.
- [3] T. Efferth and E. Koch, "Complex interactions between phytochemicals. the multi-target therapeutic concept of phytotherapy," *Curr. Drug Targets*, vol. 12, no. 1, pp. 122–132, 2011.
- [4] M. A. Kuhn, "Herbal remedies: Drug-herb interactions," *Crit. Care Nurse*, vol. 22, no. 2, pp. 22–32, 2002.

- [5] Q. Meng and K. Liu, "Pharmacokinetic interactions between herbal medicines and prescribed drugs: Focus on drug metabolic enzymes and transporters," *Curr. Drug Metab.*, vol. 15, no. 8, pp. 791–807, 2014
- [6] Jing-Jing Wu et al., "Interactions between phytochemicals from traditional chinese medicines and human cytochrome P450 enzymes," *Curr. Drug Metab.*, vol. 13, no. 5, pp. 599–614, 2012.
- [7] M. Jiang et al., "Clinical studies with traditional chinese medicine in the past decade and future research and development," *Planta Medica*, vol. 76, no. 17, pp. 2048–2064, 2010.
- [8] J. Zhang, B. Wider, H. Shang, X. Li, and E. Ernst, "Quality of herbal medicines: Challenges and solutions," *Complement. Therapies Med.*, vol. 20, no. 1-2, pp. 100–106, 2012.
- [9] J. Wei, L. Zhuo, S. Pan, X. Lian, X. Yao, and X. Fu, "Headtailtransfer: An efficient sampling method to improve the performance of graph neural network method in predicting sparse ncRNA–protein interactions," *Comput. Biol. Med.*, vol. 157, 2023, Art. no. 106783.
- [10] Z. Zhou et al., "MHAM-NPI: Predicting ncRNA-protein interactions based on multi-head attention mechanism," *Comput. Biol. Med.*, vol. 163, 2023, Art. no. 107143.
- [11] Z. Zhou, L. Zhuo, X. Fu, J. Lv, Q. Zou, and R. Qi, "Joint masking and self-supervised strategies for inferring small molecule-miRNA associations," Mol. Ther.-Nucleic Acids, vol. 35, no. 1, 2024.
- [12] L. Xu et al., "SGAE-MDA: Exploring the MiRNA-disease associations in herbal medicines based on semi-supervised graph autoencoder," *Methods*, vol. 221, pp. 73–81, 2024.
- [13] J. Xu et al., "Graph embedding and Gaussian mixture variational autoencoder network for end-to-end analysis of single-cell RNA sequencing data," *Cell Rep. Methods*, vol. 3, no. 1, 2023.
- [14] W. Liu, T. Tang, X. Lu, X. Fu, Y. Yang, and L. Peng, "MPCLCDA: Predicting circRNA-disease associations by using automatically selected meta-path and contrastive learning," *Brief. Bioinf.*, vol. 24, no. 4, 2023, Art. no. bbad227.
- [15] T. Wang, Z. Li, L. Zhuo, Y. Chen, X. Fu, and Q. Zou, "MS-BACL: Enhancing metabolic stability prediction through bond graph augmentation and contrastive learning," *Brief. Bioinf.*, vol. 25, no. 3, 2024, Art. no. bbae127.
- [16] X. Ma, X. Fu, T. Wang, L. Zhuo, and Q. Zou, "GraphADT: Empowering interpretable predictions of acute dermal toxicity with multi-view graph pooling and structure remapping," *Bioinformatics*, vol. 40, no. 7, 2024, Art. no. btae438.
- [17] T. Wang, Z. Du, L. Zhuo, X. Fu, Q. Zou, and X. Yao, "MultiCBlo: Enhancing predictions of compound-induced inhibition of cardiac ion channels with advanced multimodal learning," *Int. J. Biol. Macromolecules*, vol. 276, 2024, Art. no. 133825.
- [18] R. Wang et al., "Diff-AMP: Tailored designed antimicrobial peptide framework with all-in-one generation, identification, prediction and optimization," *Brief. Bioinf.*, vol. 25, no. 2, 2024, Art. no. bbae078.
- [19] Z. Li et al., "Multi-source data integration for explainable miRNA-driven drug discovery," *Future Gener. Comput. Syst.*, vol. 160, pp. 109–119, 2024.
- [20] Z. Zhou, L. Zhuo, X. Fu, and Q. Zou, "Joint deep autoencoder and subgraph augmentation for inferring microbial responses to drugs," *Brief. Bioinf.*, vol. 25, no. 1, 2024, Art. no. bbad483.
- [21] Z. Zhou et al., "Revisiting drug-protein interaction prediction: A novel global-local perspective," *Bioinformatics*, vol. 40, no. 5, 2024, Art. no. btae271.
- [22] J. Wei, Y. Zhu, L. Zhuo, Y. Liu, X. Fu, and F. Li, "Efficient deep model ensemble framework for drug-target interaction prediction," *J. Phys. Chem. Lett.*, vol. 15, no. 30, pp. 7681–7693, 2024.
- [23] G. Han, L. Peng, A. Ding, Y. Zhang, and X. Lin, "CTF-DDI: Constrained tensor factorization for drug–drug interactions prediction," *Future Gener. Comput. Syst.*, vol. 161, pp. 26–34, 2024.
- [24] Y. Hong et al., "DDID: A comprehensive resource for visualization and analysis of diet-drug interactions," *Brief. Bioinf.*, vol. 25, no. 3, 2024, Art. no. bbae212.
- [25] Y.-S. Cho, "Decoupled variational graph autoencoder for link prediction," in *Proc. ACM Web Conf.*, 2024, pp. 839–849.
- [26] A. Radford et al., "Learning transferable visual models from natural language supervision," in *Proc. Int. Conf. Mach. Learn.*, 2021, pp. 8748–8763.
- [27] J. An, W. Ding, and J. Lin, "ChatGPT," Tackle Growing Carbon Footprint Generative AI, vol. 615, p. 586, 2023. [Online]. Available: https://doi.org/ 10.1038/d41586-023-00843-2
- [28] D. J. Beal, "ESM 2.0: State of the art and future potential of experience sampling methods in organizational research," *Annu. Rev. Organ. Psychol. Organ. Behav.*, vol. 2, no. 1, pp. 383–407, 2015.

- [29] Y. Dong, S. Wang, Y. Wang, T. Derr, and J. Li, "On structural explanation of bias in graph neural networks," in *Proc. 28th ACM SIGKDD Conf. Knowl. Discov. Data Mining*, 2022, pp. 316–326.
- [30] Y. Bai, J. Mei, A. L. Yuille, and C. Xie, "Are transformers more robust than CNNS?," in *Proc. Adv. Neural Inf. Process. Syst.*, 2021,vol. 34, pp. 26831–26843.
- [31] Y. Yang, Y. Rao, M. Yu, and Y. Kang, "Multi-layer information fusion based on graph convolutional network for knowledge-driven herb recommendation," *Neural Netw.*, vol. 146, pp. 1–10, 2022.
- [32] K. Islam, S. Aridhi, and M. Smail-Tabbone, "A comparative study of similarity-based and GNN-based link prediction approaches," in *Proc. Graph Embedding Mining Workshop*, Sep. 2020.
- [33] A. Salehi and H. Davulcu, "Graph attention auto-encoders," in *Proc. IEEE 32nd Int. Conf. Tools Artif. Intell.*, Nov. 2020, pp. 989–996.
- [34] Thomas N. Kipf and M. Welling, "Variational graph auto-encoders," 2016, arXiv:1611.07308.
- [35] F. D. Giovanni, J. Rowbottom, B. P. Chamberlain, T. Markovich, and M. M. Bronstein, "Graph neural networks as gradient flows: Understanding graph convolutions via energy," in *Proc. Int. Conf. Learn. Representations*, 2023.
- [36] J. S. Ahn and M. H. Kim, "Variational graph normalized autoencoders," in *Proc. 30th ACM Int. Conf. Inf. Knowl. Manage.*, 2021, pp. 2827–2831.
- [37] B. T. Knapik, A. W. Van Der Vaart, and J. H. van Zanten, "Bayesian inverse problems with Gaussian priors," *Ann. Statist.*, vol. 39, no. 5, pp. 2626–2657, 2011.

- [38] S. Lee et al., "Stochastic multiple choice learning for training diverse deep ensembles," Adv. Neural Inf. Process. Syst., vol. 29, 2016.
- [39] G. J. McLachlan and T. Krishnan. *The EM Algorithm and Extensions*. Hoboken, NJ, USA: Wiley, 2008.
- [40] T. N. Kipf and M. Welling, "Semi-supervised classification with graph convolutional networks," in *Proc. Int. Conf. Learn. Representations*, 2022.
- [41] P. Veličković, G. Cucurull, A. Casanova, A. Romero, P. Liò, and Y. Bengio, "Graph attention networks," in *Proc. Int. Conf. Learn. Representations*, 2018
- [42] Y. Wang, Y. Zhai, Y. Ding, and Q. Zou, "SBSM-Pro: Support bio-sequence machine for proteins," Sci. China Inf. Sci., vol. 67, no. 11, 2024, Art. no. 212106.
- [43] J. Wei et al., "DrugReAlign: A multisource prompt framework for drug repurposing based on large language models," *BMC Biol.*, vol. 22, no. 1, 2024, Art. no. 226.
- [44] J. Wei et al., "BloodPatrol: Revolutionizing blood cancer diagnosis-advanced real-time detection leveraging deep learning & cloud technologies," *IEEE J. Biomed. Health Informat.*, early access, Nov. 11, 2024, doi: 10.1109/JBHI.2024.3496294.
- [45] G. Di Carlo, F. Borrelli, E. Ernst, and A. A. Izzo, "St John's wort: Prozac from the plant kingdom," *Trends Pharmacological Sci.*, vol. 22, no. 6, pp. 292–297, 2001.
- [46] K. Linde, M. M. Berner, and L. Kriston, "St John's wort for major depression," *Cochrane Database Systematic Rev.*, vol. 4, 2008.